






Synergistic action between a synthetic cannabinoid compound and tramadol in neuropathic pain rats

GEOVANNA NALLELY QUIÑONEZ-BASTIDAS^{1,*} 
ULISES OSUNA-MARTÍNEZ² 
ANA LAURA REDA-LICEA²
MANUEL LÓPEZ-ORTÍZ³ 
IGNACIO REGLA³ 
ANDRÉS NAVARRETE^{1,3*} 

¹ *Facultad de Química, Departamento de Farmacia, Universidad Nacional Autónoma de México, Ciudad Universitaria Coyoacán, Ciudad de México, México*

² *Facultad de Ciencias Químico-Biológicas Laboratorio de Investigación en Farmacia Farmacobiología y Toxicobiología Universidad Autónoma de Sinaloa Av. de las Américas y Boulevard Universitarios, Culiacán, Sinaloa, 80010 Mexico*

³ *Facultad de Estudios Superiores Zaragoza Universidad Nacional Autónoma de México (UNAM), México, D.F., México*

ABSTRACT

In the present study the interaction of cannabinoid, PhAR-DBH-Me [(*R,Z*)-18-((1*S*,4*S*)-5-methyl-2,5-diazabicyclo[2.2.1]heptan-2-yl)-18-oxooctadec-9-en-7-yl]phenylacetate] and tramadol in two neuropathy models, as well as their possible toxic effects, was analyzed. The anti-allodynic effect of PhAR-DBH-Me, tramadol, or their combination, were evaluated in neuropathic rats. Furthermore, the effective dose 35 (as the 35 % of the antiallodynic effect) was calculated from the maximum effect of each drug. Moreover, the isobolographic analysis was performed to determine the type of interaction between the drugs. A plasma acute toxicity study was carried out to assess the hepatic, renal, and heart functions after an individual or combined administration of the drugs, as well as histology using the hematoxylin-eosin or Masson-trichrome method. PhAR-DBH-Me, tramadol, and their combination produced an antiallodynic effect on spinal nerve ligation (SNL) and cisplatin-induced neuropathic pain in rats. Moreover, PhAR-DBH-Me and tramadol combination showed a synergistic interaction in neuropathic pain rats induced by SNL but not for cisplatin-induced neuropathy. On the other hand, changes in renal and hepatic functions were not observed. Likewise, analysis of liver, kidney and heart histology showed no alterations compared with controls. Results show that the combination of PhAR-DBH-Me and tramadol attenuates the allodynia in SNL rats; the acute toxicology analysis suggests that this combination could be considered safe in administered doses.

Keywords: cannabinoid receptors, PhAR-DBH-Me, tramadol, synergism, antiallodynic effect

Accepted April 21, 2022
Published online April 21, 2022

INTRODUCTION

Recent reports indicate that cannabinoid-based therapy of pain can be used to reduce the global problem of opioid use (1). Opioid and cannabinoid endogenous systems have a role in modulating several presynaptic and postsynaptic pathways related to pain control.

* Correspondence; e-mail: anavarrt@unam.mx; geovanna_quinonez@quimica.unam.mx

Reports have also suggested the interaction between both systems at peripheral, spinal and supraspinal levels (2–4). Cannabinoid and opioid receptors are coupled to Gi protein receptors. After their activation, Gi signaling pathway decreases intracellular cAMP levels, producing activation of voltage-gated potassium channels and closure of calcium channels. These mechanisms reduce the pro-nociceptive-type neurotransmitters released from presynaptic nerve terminals to induce antinociception (5). Moreover, reports indicate a bidirectional interaction between cannabinoid and opioid system, heteromeric conformations by cannabinoid and opioid receptors (CB1- μ opioid receptor, heteromeric complex), as well as a beta-endorphin release after CB2 receptor activation (6–8). On the other hand, studies demonstrated that concomitant use of opioid and cannabinoid drugs induces synergic interaction to relieve the pain (9–12). It was previously shown that (*R,Z*)-18-((1*S*,4*S*)-5-methyl-2,5-diazabicyclo[2.2.1]heptan-2-yl)-18-oxooctadec-9-en-7-ylphenylacetate (PhAR-DBH-Me), a synthetic cannabinergic compound, produced an antiallodynic effect in neuropathic rats (13) through the partial activation of CB1/CB2 receptors, and full activation of TRPV1 channels. Considering that synergistic interactions are produced from different antinociceptive pathways, it has been hypothesized that interaction between a novel cannabinergic compound, PhAR-DBH-Me, and tramadol, an opioid agonist with an effect on serotonergic and noradrenergic transmission, may provide a valuable opportunity to treat allodynia-like behavior in neuropathic rats.

As far as we know there is no previous report about the synergistic antiallodynic action of combined PhAR-DBH-Me and tramadol. Hence, the aim of this study was to evaluate the interaction between PhAR-DBH-Me and tramadol on allodynic rats (SNL and cisplatin models), as well as to determine if the systemic administration of this combination produces alterations in the liver, kidneys, and heart in the treated animals.

EXPERIMENTAL

Animals and experimental design

Eight weeks old female Wistar rats weighing 160–180 g were acquired from Centro UNAM-Envigo (Envigo México, S.A. de C.V., Mexico) and maintained in a temperature-controlled room on a 12-h light/dark cycle with food (Lab diet, 5012, Purina, Mexico) and water *ad libitum* throughout the study. All procedures were performed in accordance with National and International Guidelines for Care and Use of Laboratory Animals, NOM-062-ZOO-1999, and National Research Council, resp., and were approved by the Ethics Committee for the Use of Animals in Pharmacological and Toxicological Testing (Faculty of Chemistry, UNAM Ciudad de México, México). The experimental design included a total of 216 rats distributed in thirty-six independent groups (Table I).

Drugs

(*R,Z*)-18-((1*S*,4*S*)-5-methyl-2,5-diazabicyclo[2.2.1]heptan-2-yl)-18-oxooctadec-9-en-7-ylphenylacetate was synthesized by Lopez-Ortiz (14). Commercial solution for injection of tramadol hydrochloride (100 mg in 2 mL, AMSA Laboratories, Mexico) was used and doses of 1, 3.2, 10, 32, and 56 mg were taken directly from that solution. Both drugs were administered intraperitoneally.

Table I. Experimental design and groups

Group (<i>n</i> = 6)	Treatment (mg kg ⁻¹ , <i>i. p.</i>)	Group (<i>n</i> = 6)	Treatment (mg kg ⁻¹ , <i>i. p.</i>)
Logarithmic dose-response curve of antiallodynic effect			
SNL	PhAR-DBH-Me: 3.2	Cis	PhAR-DBH-Me: 3.2
SNL	PhAR-DBH-Me: 10	Cis	PhAR-DBH-Me: 10
SNL	PhAR-DBH-Me: 32	Cis	PhAR-DBH-Me: 32
SNL	PhAR-DBH-Me: 100	Cis	PhAR-DBH-Me: 100
SNL	Tramadol: 3.2	Cis	Tramadol: 1
SNL	Tramadol: 10	Cis	Tramadol: 3.2
SNL	Tramadol: 32	Cis	Tramadol: 10
SNL	Tramadol: 56	Cis	Tramadol: 32
MEP (%) of combinations			
Sham	Veh	Veh	Veh
SNL	Veh	Cis	Veh
SNL-C1	Combination 1	Cis-C1	Combination 1
	[PhAR-DBH-Me:tramadol]: 24.88:12.42		[PhAR-DBH-Me:tramadol]: 18.57:2.27
SNL-C2	Combination 2	Cis-C2	Combination 2
	[PhAR-DBH-Me:tramadol]: 12.44:6.21		[PhAR-DBH-Me:tramadol]: 9.285:1.135
SNL-C3	Combination 3	Cis-C3	Combination 3
	[PhAR-DBH-Me:tramadol]: 6.22:3.10		[PhAR-DBH-Me:tramadol]: 4.64:0.567
SNL-C4	Combination 4	Cis-C4	Combination 4
	[PhAR-DBH-Me:tramadol]: 3.11:1.55		[PhAR-DBH-Me:tramadol]: 2.32:0.83
Toxicology assay groups			
SNL	Veh	Cis	Veh
SNL	ED ₃₅ PhAR-DBH-Me: 49.79	Cis	ED ₃₅ PhAR-DBH-Me: 37.13
SNL	ED ₃₅ tramadol: 24.85	Cis	ED ₃₅ Tramadol: 4.54
SNL-C1	Combination 1: 24.88:12.42	Cis-C1	Combination 1: 18.57/2.27

Veh – vehicle, saline

Cisplatin (Cis), solution for injection (50 mg in 50 mL, Pisa Laboratories, Mexico) was used for inducing neuropathy at a dose of 0.1 mg kg⁻¹, *i. p.*

Doses of PhAR-DBH-Me and tramadol for constructing dose-response curves, as well as doses of cisplatin used to induce neuropathy, were established in accordance with our previous study (13).

Induction of neuropathy and allodynia assessment

Two well-known models to produce allodynia were used: spinal nerve ligation (SNL) (15) and the chemotherapy model, based on repeated injections of cisplatin (0.1 mg kg⁻¹) every third day for 15 days (16). SNL rats were submitted to surgical procedure, L5 and L6 spinal nerves were exposed and tightly ligated with a 6-0 silk structure distal to the dorsal root ganglion, whereas for sham rats the nerves were exposed but not ligated.

Tactile allodynia was evaluated by the Chaplan method (17) using a recently developed rat surgical neuropathy model wherein nocifensive behaviors are evoked by light touch to the paw. Employing von Frey hairs from 0.41 to 15.1 g, we first characterized the percent response at each stimulus intensity. A smooth log-linear relationship was observed, with a median 50 % threshold at 1.97 g (95 % confidence limits, 1.12-3.57 g which consists in using calibrated von Frey filaments (Stoelting Co., USA), in a range of 0.4 to 15 g, to produce six different positive or negative tactile responses in the plantar paw of the rat. The rats with values less than 4 g were considered allodynic. Allodynia was measured for 8 hours and then the area under the curve was calculated to obtain the percentage of maximum possible effect (MPE, %) as previously described (13):

$$\text{MPE (\%)} = \frac{AUC_{\text{compd}} - AUC_{\text{sham}}}{AUC_{\text{sham}} - AUC_{\text{veh}}} \times 100 \quad \text{Eq. 1}$$

Isobolographic analysis

Initially, both SNL and Cis rats were given increased doses of PhAR-DBH-Me (3.2, 10, 32, and 100 mg kg⁻¹), and tramadol for SNL (3.2, 10, 32, and 56 mg kg⁻¹) and Cis rats (1, 3.2, 10, 32 mg kg⁻¹).

The type of interaction between PhAR-DBH-Me and tramadol was evaluated by the isobolographic analysis (18, 19). In order to complete the objective, the effective dose (ED_{35})-response for PhAR-DBH-Me and tramadol was determined using the Hill equation (20).

The theoretical additive doses (Z_{ad}) with their standard error (SEM) for the combination of drugs 1:1 was computed from the effective doses 35 (ED_{35}) of the single drugs, according to the procedure described by Tallarida (18, 19):

$$Z_{ad} = f \times A + (1 - f) \times B \quad \text{Eq. 2}$$

where A is ED_{35} of PhAR-DBH-Me and B was ED_{35} of tramadol, whereas that, $f = 0.5$ (according to proportion 1:1).

Moreover, a proportion of drugs [0.5 ED_{35} of PhAR-DBH-Me : 0.5 ED_{35} of tramadol (theoretical additive dose, Z_{ad})] was fixed to construct four different combinations as follows: (0.5 ED_{35} PhAR-DBH-Me + 0.5 ED_{35} tramadol)/2, (0.5 ED_{35} PhAR-DBH-Me + 0.5 ED_{35} tramadol)/4, (0.5 ED_{35} PhAR-DBH-Me + 0.5 ED_{35} tramadol)/8 and (0.5 ED_{35} PhAR-DBH-Me + 0.5 ED_{35} tramadol)/16. A dose-response curve was then constructed and $ED_{35\text{exp}}$ of the combination was determined. In addition, the interaction index (γ) was calculated:

$$\gamma = ED_{35\text{exp}} / ED_{35\text{theor}} \quad \text{Eq. 3}$$

value close to 1 indicates no interaction ($ED_{35\text{exp}} \approx ED_{35\text{theor}}$), whereas values higher than 1 ($ED_{35\text{exp}} > ED_{35\text{theor}}$) represent antagonism and lower than 1 ($ED_{35\text{exp}} < ED_{35\text{theor}}$) represent a synergistic interaction. *t*-Student test-based statistical analysis which incorporates some adaptations for the isobolographic analysis was applied, where *t'* value was determined from:

$$t' = \frac{M}{\sqrt{[(SE(\log Z_{\text{ad}}))^2 + (SE(\log Z_{\text{ex}}))^2]}} \quad \text{Eq. 4}$$

where, Z_{ad} is the theoretical additive dose, and Z_{ex} is the experimental dose, $M = \log Z_{\text{ad}} - \log Z_{\text{ex}}$ with respective standard errors on the log scale, because Z_{ad} and Z_{ex} are log-normally distributed (18). Then, the value of *t'* was compared with the *T* value:

$$T = \frac{t_{\text{ad}}(SE(\log Z_{\text{ad}}))^2 + t_{\text{ex}}(SE(\log Z_{\text{ex}}))^2}{SE(\log Z_{\text{ad}})^2 + SE(\log Z_{\text{ex}})^2} \quad \text{Eq. 5}$$

t_{ad} value was obtained from the *t*-Student distribution table with degrees of freedom, where n_1 and n_2 represent the number of data used in the regression analysis for drug 1, PhAR-DBH-Me, and drug 2, tramadol. t_{ex} was obtained from the same table with $n_{\text{ex}} - 2$ degrees of freedom, where n_{ex} is the number of data used in the regression analysis to calculate the Z_{ex} of the combination. If $|t'| > T$, there is a significant difference between theoretical (Z_{ad}) and experimental (Z_{ex}) data (19).

Toxicology assays: hepatic, renal and cardiac damage profile

Animals were administered with an overdose of sodium pentobarbital (150 mg kg⁻¹, *i.p.*) and a blood sample was obtained by cardiac puncture and deposited in microtubes with heparin. Samples were immediately centrifuged at 5000 rpm for 5 min, at 4 °C. Once centrifuged, 200 µL of the supernatant (plasma) were taken and deposited in a disk of diagnosis plus panel (Skyla Corp. H.S.P.B, Taiwan), and the disk was placed into HB1 Clinical Chemistry Analyzer (Skyla V B1) for the analysis of albumin/globulin ratio, blood ureic nitrogen/creatinine ratio, #C-Ca (creatinine-calcium), globulin, Na/K, urea, albumin, alkaline phosphatase, alanine transaminase, amylase, blood ureic nitrogen (BUN), creatinine, Ca, glucose, K, Na, phosphate, bilirubin and total protein.

Histology

Liver, kidney, and heart were collected 24 h after rats were treated and then washed with saline solution, 0.9 %, to remove the excess blood. Immediately, tissues were placed in 50-mL Falcon tubes containing 10 % formalin (J. T. Baker, USA), 0.4 % NaH₂PO₄ (Vetec, USA), and 0.65 % Na₂HPO₄ (Fermont, Mexico); then, the solution was adjusted to pH 7.4. The tissue was slit into 0.5 × 2.0 cm pieces and embedded in paraffin (Leica Paraplast, USA). Subsequently, the samples were cut using a microtome (Leica RM2125 RTS, Leica Biosystems, USA) with a thickness of 5–7 µm, placed on 2 slides per sample and stained with hematoxylin and eosin (H&E) for cellular analysis, or Masson trichrome (MT) for the evaluation of the distribution and structure of collagen (21, 22).

Statistical analysis

Data are presented as a mean \pm standard error of the mean (SEM) for 6 animals. The dose-response curve was constructed using the area under the curve obtained through the trapezoidal method. Data were expressed as the percentage of maximum possible effect (MPE, %).

Differences were tested by one-way analysis of variance (ANOVA), followed by Tukey's test with $p \leq 0.05$ indicating statistical significance. To determine the interaction type between drugs, $t' > T$, was considered a synergistic interaction. The results were analyzed using the statistical software Sigma plot (version 12.0). Tables and figures were designed using Graph-Pad Prism (version 6.0).

RESULTS AND DISCUSSION

Interaction between PhAR-DBH-Me and tramadol

Interaction type between PhAR-DBH-Me and tramadol in two different models: spinal nerve ligated rats and Cis-induced neuropathic rats was examined in the present study.

Spinal nerve ligated rats. – All intraperitoneal treatments, PhAR-DBH-Me, at doses of 3.2, 10, 32, and 100 mg kg⁻¹, or tramadol, at doses of 3.2, 10, 32, and 56 mg kg⁻¹ produced an antiallodynic effect in SNL rats (Fig. 1a). ED_{35} of antiallodynic effect was 49.77 ± 0.06 and 24.85 ± 0.05 mg kg⁻¹ for PhAR-DBH-Me and tramadol, resp., when administered separately. Intraperitoneal administration of a series of combinations of PhAR-DBH-Me and tramadol (in mg kg⁻¹, for the groups see Table I) of 24.88:12.42 (SNL-C1), 12.44:6.21 (SNL-C2), 6.22:3.10 (SNL-C3), and 3.11:1.55 (SNL-C4), produced significant ($p \leq 0.05$) antiallodynic effect in neuropathic rats (Fig. 1b). Results demonstrated that the combination in group SNL-C1 was the most effective to reach an antiallodynic effect (46.2 %) in SNL rats. Once evaluated the four combinations, the isobologram was constructed. An oblique line, a theoretical line, was plotted to join the ED_{35} of PhAR-DBH-Me (dark point on the X-axis) and ED_{35} of tramadol (dark point on the Y-axis) (Fig. 1c). Afterwards, the theoretical point ($24.88 \pm 0.05 : 12.43 \pm 0.23$, PhAR-DBH-Me:tramadol, mg kg⁻¹) was fixed in the middle of the oblique line of the isobologram (white circle), whereas the experimental point ($5.72 \pm 0.51 : 2.86 \pm 0.25$ mg kg⁻¹, PhAR-DBH-Me:tramadol) was localized under the oblique line (grey point), near to the intersection of axes (Fig. 1c). Isobologram showed that the experimental dose of the combination was lower than the theoretical dose. Moreover, the isobolographic analysis indicated an interaction index value (γ) of 0.23020 for the PhAR-DBH-Me and tramadol combination. Additionally, the interaction type between both drugs corroborated with the differences between t' and T ($t' = 9.4582 > T = 3.4422$) (Fig. 1c), indicating a synergistic type of interaction (18, 19).

To the best of our knowledge, this is the first report about the synergistic antinociceptive action of the PhAR-DBH-Me and tramadol combination. However, previous studies suggested that morphine and CB2 agonist, WIN55212, when combined produced a synergistic interaction in a chronic constriction injury lesion in mice (23). To support our results, *N*-palmitoylethanolamide (PEA), an endogenous cannabinoid analog of anandamide, and tramadol combination demonstrated a synergistic anti-nociceptive effect in a formalin

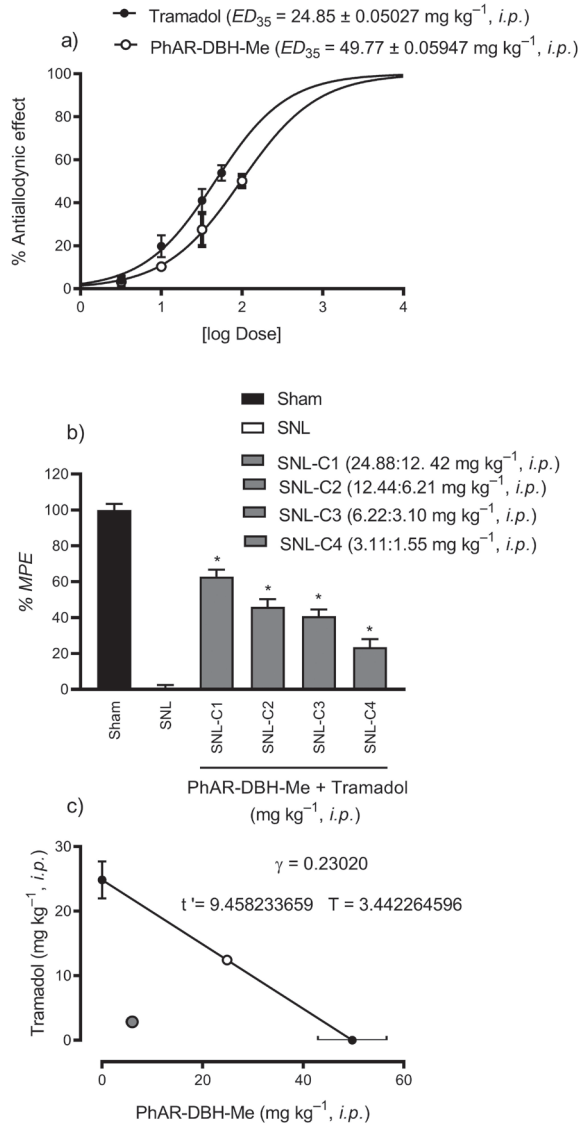


Fig. 1. Synergistic interaction between PhAR-DBH-Me and tramadol in spinal nerve ligation-induced allodynia in rats. a) Logarithmic dose-response curve of antiallodynic effect induced by PhAR-DBH-Me (3.2, 10, 32 and 100 $\text{mg kg}^{-1}, i.p.$) and tramadol (3.2, 10, 32 and 56 $\text{mg kg}^{-1}, i.p.$). b) Maximum possible effect (MPE, %) of antiallodynia reached by administration combinations (24.88:12.42, 12.44:6.21, 6.22:3.10, 3.11:1.55 $\text{mg kg}^{-1}, i.p.$) of PhAR-DBH-Me and tramadol in groups of SNL-C1 to SNL-C4. c) ED_{35} for PhAR-DBH-Me ($49.79 \pm 0.05 \text{ mg kg}^{-1}, i.p.$, X-axis) vs. ED_{35} tramadol ($24.85 \pm 0.05 \text{ mg kg}^{-1}, i.p.$, Y-axis); black points, bars indicate SEM, $n = 6$. White and grey circle indicate the theoretical ($24.88 \pm 0.05:12.43 \pm 0.23 \text{ mg kg}^{-1}, i.p.$, PhAR-DBH-Me:tramadol) and experimental point ($5.72 \pm 0.51: 2.86 \pm 0.25 \text{ mg kg}^{-1}, i.p.$, PhAR-DBH-Me:tramadol).

mice model (24). A synergistic effect occurs when substances combine two or more specific mechanisms of anti-nociceptive pathways, relevant for pain processing. Previous studies reported that PhAR-DBH-Me activated CB1, CB2, and TRPV1 receptors (13). Moreover, tramadol activates mu-opioid and serotonergic receptors, with an inhibitory effect on ascending and descending inhibitory pain pathways (13, 25). Therefore, opioid and cannabinoid combination could be a new therapeutic approach to minimize the undesirable side-effects and limitations of each drug treatment used in a separate scheme. On the other hand, pharmacokinetic interactions are important in drug-drug interactions. Since PhAR-DBH-Me is a synthetic compound that mimics anandamide and the hepatic metabolism of anandamide involves CYP3A4, 2D6 and 4F2C (26–28), whereas tramadol is mainly metabolized by CYP2D6, CYP2B6 and CYP3A4 (29), a study of the pharmacokinetic interaction between PhAR-DBH-Me and tramadol might be considered in the future.

Cisplatin-induced neuropathic rats. – After a repeated dose of cisplatin (0.1 mg kg^{-1} , *i.p.*) the rats developed tactile allodynia, which was reversed by the acute treatment with increased doses of PhAR-DBH-Me (3.2, 10, 32 and 100 mg kg^{-1}) and tramadol (1, 3.2, 10, 32 mg kg^{-1}). ED_{35} of the antiallodynic effect of each drug was 37.14 ± 0.06 and $4.54 \pm 0.06 \text{ mg kg}^{-1}$ for PhAR-DBH-Me and tramadol, resp. (Fig. 2a). The differences between the ED_{35} s of PhAR-DBH-Me and tramadol, calculated for SNL- and cisplatin-induced models, could be due to the characteristics of each neuropathic model of pain. Once calculated, ED_{35} of each drug was fixed and a series of combinations for PhAR-DBH-Me:tramadol (in mg kg^{-1} ; for experimental groups see Table I) of 18.57:2.27 (Cis-C1), 9.285:1.135 (Cis-C2), 4.64:0.567 (Cis-C3), 2.32:0.83 (Cis-C4) were prepared (Fig. 2b). All combinations produced an antiallodynic effect. However, only Cis-C1 and Cis-C2 groups were significantly different ($p \leq 0.05$). Then, an isobologram was constructed from ED_{35} of tramadol (dark point on the Y-axis) and ED_{35} of PhAR-DBH-Me (dark point on the X-axis), and both points were joined by an oblique line or theoretical line. Then, were fixed the theoretical additive point, a white circle, ($18.58 \pm 2.82 : 2.27 \pm 0.34 \text{ mg kg}^{-1}$, PhAR-DBH-Me:tramadol), in the middle of an oblique line, and the experimental point, a grey circle ($13.17 \pm 0.55 : 1.61 \pm 0.06 \text{ mg kg}^{-1}$, PhAR-DBH-Me:tramadol), under the additive line (Fig. 2c). Moreover, from the relation between the theoretical dose and experimental dose of combinations, the interaction index was calculated, $\gamma = 0.7095$; the values near 1 indicate a probable simple additive relationship, as this index is calculated from the relation: experimental dose/theoretical dose. Besides, a comparison between t' and T ($t' = 0.0058$ and $T = 3.479$) confirmed that PhAR-DBH-Me and tramadol had an antiallodynic additive effect in cisplatin-induced neuropathy in rats (Fig. 2c). In contrast with the SNL model, data suggest that combination PhAR-DBH-Me:tramadol, causes no synergistic effect in cisplatin-induced neuropathy rats.

Cannabinoid therapy has been already reported for its effectivity in cisplatin models (30), and some reports indicated that co-expression of cannabinoid and opioid receptors are necessary for analgesic effects (31). Several studies suggested the presence of cannabinoid-opioid heteromers, as well as β -endorphin release exerted by CB2 activation (6–8). Then, CB1 antagonism reversed the μ -opioid-induced analgesia in an inflammatory pain model (32). Hence, there is a bi-directional relationship in the regulation of both antiallodynic systems. Modulatory effects between cannabinoids and μ -opioid receptors have been observed in clinical studies as well in which opioid and cannabinoid combination produced a synergistic analgesic effect and attenuated the development of opioid tolerance (33).

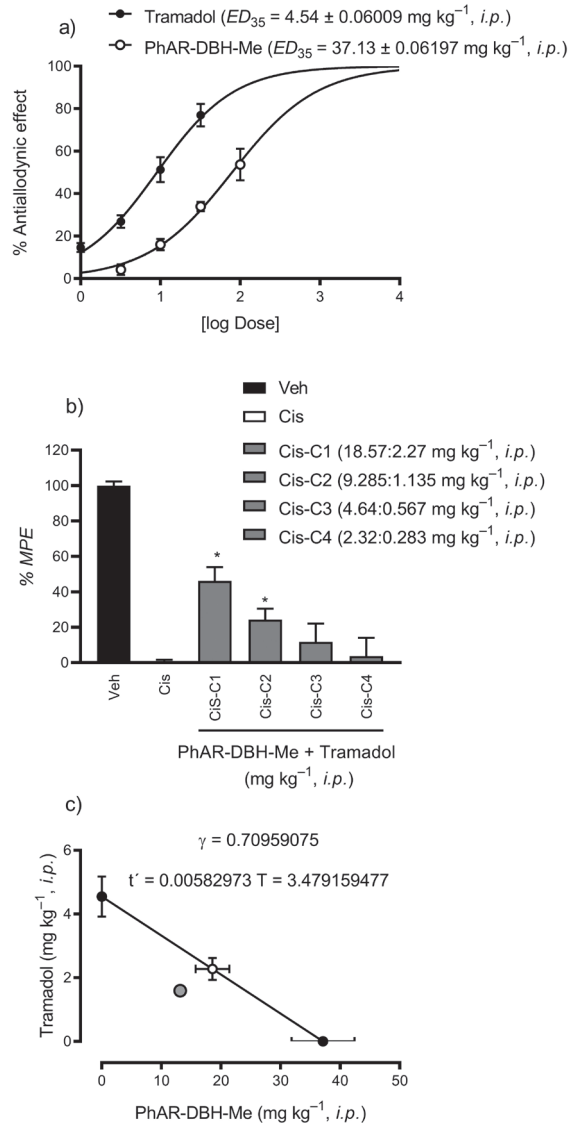


Fig. 2. Synergistic interaction between PhAR-DBH-Me and tramadol combination in cisplatin-induced allodynia in rats. a) Logarithmic dose-response curve of antiallodynic effect induced by PhAR-DBH-Me (3.2, 10, 32 and 100 mg kg⁻¹, *i.p.*) and tramadol (1, 3.2, 10 and 32 mg kg⁻¹, *i.p.*). b) Maximum possible effect (MPE, %) of antiallodynia reached by administration of combinations (18.57:2.27, 9.285:1.135, 4.64:0.567, 2.32:0.83 mg kg⁻¹, *i.p.*) of PhAR-DBH-Me and tramadol in groups Cis-C1 to Cis-C4. c) ED_{35} for PhAR-DBH-Me ($37.13 \pm 0.06 \text{ mg kg}^{-1}, i.p.$, X-axis) and ED_{35} tramadol ($4.54 \pm 0.6 \text{ mg kg}^{-1}, i.p.$, Y-axis), bars indicate SEM, $n = 6$. White and grey circles indicate the theoretical ($18.58 \pm 2.82:2.27 \pm 0.34 \text{ mg kg}^{-1}, i.p.$, PhAR-DBH-Me:tramadol) and experimental point ($13.17 \pm 0.55: 1.61 \pm 0.06 \text{ mg kg}^{-1}, i.p.$, PhAR-DBH-Me:tramadol).

Hepatic, renal and cardiac damage

Effect of systemic administration of PhAR-DBH-Me, tramadol and their combination. – After 24 hours of a single administration of ED_{35} of PhAR-DBH-Me or tramadol or their combination in SNL-C1, blood biomarkers did not exert significant changes (Table II), when compared with the control group. This suggested that ED_{35} after acute administration of PhAR-DBH-Me and tramadol or their combination in SNL-C1 did not produce hepatic, renal and cardiac damage in the SNL neuropathy model. Amylase values were significantly higher ($p \leq 0.05$) for ED_{35} PhAR-DBH-Me (180.28 ± 6.16 U per 100 mL) and SNL-C1 (184.28 ± 9.92 U per 100 mL) treated rats compared with vehicle (133 ± 5.18 U per 100 mL) or ED_{35} tramadol (132 ± 6.20 U per 100 mL) groups (Table II). Such releasing of amylase could be suggesting the damage in the pancreas as well as impaired hepatic or renal microcirculation (34), however, there was no evidence of histopathological damage.

Likewise, the changes in albumin and globulin proteins are indicators of early diagnosis or prognostic information for some diseases (35). In our study, we observed significantly ($p \leq 0.05$) increased levels of proteins in cisplatin-induced neuropathic rats; albumin/globulin ratio for tramadol (2.17 ± 0.08), PhAR-DBH-Me (2.12 ± 0.64) and Cis-C1 (2.09 ± 0.13) in treated animals was higher compared with the vehicle group (1.54 ± 0.04). Moreover, globulin levels (g per 100 mL) were significant lower ($p \leq 0.05$) for tramadol, PhAR-DBH-Me and Cis-C1 group (1.98 ± 0.05 , 2.07 ± 0.05 , 2.05 ± 0.09 , resp.), compared with the vehicle group (2.6 ± 0.03).

The observation of impaired liver function in chronic users of cannabis was published 50 years ago (36). In this regard, acute toxicity of cannabidiol (CBD) was observed in mice treated with CBD-enriched cannabis extract, which then showed increased levels of alanine transferase, aspartate transferase, total bilirubin and glutathione (37)246, 738, or 2460 mg/kg of CBD (acute toxicity, 24 h. However, we did not observe changes in the mentioned hepatic biomarkers in our study. Furthermore, proteinuria, an important sign of kidney damage, as well as an increased weight of kidneys, was observed in rats treated with CB1 agonist (38). In our study, biochemical blood biomarkers followed by histological observations indicated no relevant changes to be induced by the treatments.

There is consistent evidence about electrolytes being a measure for the diagnosis of renal or hepatic damage/disease (39). Na/K ratio values for tramadol (6.57 ± 1.64), PhAR-DBH-Me (25.70 ± 0.68) and Cis-C1 group (24.13 ± 1.87) (Table III) were significantly lower compared to the vehicle-treated animals (33.09 ± 0.65). Finally, a significant increase in K (mmol per 100 mL) ($p \leq 0.05$) was observed in PhAR-DBH-Me- (5.66 ± 0.16) and Cis-C1- (6.06 ± 0.48) treated rats. Electrolytic disorders could lead to impairment in renal excretion and result in cardiovascular complications (40). In this regard, reports indicated that anandamide modulated renal hemodynamics and produced a decreased glomerular filtration (41). Due to our results, the decreased Na/K ratio might be indicating sodium reduction and/or potassium increase (hyperkalemia).

A single effective dose of tramadol, PhAR-DBH-Me and their combination. – The morphological analysis of parenchyma, portal structure and central vein showed normal architecture without the presence of inflammatory infiltrate, hemorrhage, apoptotic or necrotic cells. These results were observed in liver samples of tramadol, PhAR-DBH-Me, or their combination-treated rats in both SNL (Figs. 3a–d) and cisplatin-induced models (Figs. 3e–h).

Table II. Blood plasma biomarkers from spinal nerve ligated rats

Blood plasma biomarker	Vehicle (saline solution)	ED ₃₅ tramadol (4979 mg kg ⁻¹)	ED ₃₅ PhAR-DBH-Me (24.85 mg kg ⁻¹)	PhAR-DBH-Me:tramadol (SNL-C1: 24.88:12.42 mg kg ⁻¹)
Albumin/globulin ratio	1.55 ± 0.03	1.67 ± 0.11	1.46 ± 0.05	1.57 ± 0.04
Blood ureic nitrogen/creatinine ratio	36.96 ± 1.82	36.67 ± 4.36	33.09 ± 2.71	34.53 ± 1.68
#C-Ca (mg per 100 mL)	10.69 ± 0.13	10.37 ± 0.14	10.44 ± 0.15	10.22 ± 0.00
#Globulin (g per 100 mL)	2.66 ± 0.04	2.40 ± 0.14	2.71 ± 0.08	2.47 ± 0.02
#Na/K	24.97 ± 1.54	25.82 ± 1.15	24.70 ± 1.59	26.72 ± 1.20
#Urea (mg per 100 mL)	37.57 ± 2.37	38.56 ± 2.33	35.73 ± 1.67	34.19 ± 1.67
#Albumin (g per 100 mL)	4.14 ± 0.03	4.11 ± 0.06	3.82 ± 0.07	3.94 ± 0.07
#Alkaline phosphatase (U per 100 mL)	159.75 ± 9.49	151.42 ± 9.73	158.57 ± 12.69	176.66 ± 19.14
Alanine transaminase (U per 100 mL)	47.66 ± 12.04	38.00 ± 2.12	36.85 ± 3.63	38.33 ± 10.83
Amylase (U per 100 mL)	133.00 ± 5.18	132.00 ± 6.20	180.28 ± 6.16 ^a	184.28 ± 9.92 ^a
Blood ureic nitrogen (mg per 100 mL)	18.94 ± 1.10	18.70 ± 1.09	16.70 ± 0.74	15.38 ± 0.78
Creatinine (mg per 100 mL)	0.53 ± 0.02	0.55 ± 0.04	0.52 ± 0.03	0.46 ± 0.02
Ca (mg per 100 mL)	10.83 ± 0.14	10.45 ± 0.15	10.30 ± 0.17	10.18 ± 0.18
Glucose (mg per 100 mL)	127.62 ± 10.56	95.57 ± 3.84	196.71 ± 11.27	168.42 ± 7.48
K (mmol per 100 mL)	6.02 ₅ ± 0.34	5.65 ± 0.03	6.48 ± 0.48	5.44 ± 0.26
Na (mmol per 100 mL)	146.75 ± 0.79	143.71 ± 1.69	147.42 ± 0.90	143.28 ± 0.63
Phosphate (mg per 100 mL)	8.34 ± 0.29	8.9 ± 0.4 ₅	7.51 ± 0.30	7.98 ± 0.31
Bilirubin (mg per 100 mL)	0 ± 0	0 ± 0	0 ± 0	0 ± 0
Total protein (g per 100 mL)	6.83 ± 0.50	6.51 ± 0.17	6.54 ± 0.09	6.41 ± 0.05

Mean ± SEM, *n* = 6.

^aStatistically significant difference vs. vehicle; *p* < 0.05.

Table III. Blood plasma biomarkers from cisplatin-induced rats

Blood plasma biomarker	Vehicle (saline solution)	ED ₃₅ tramadol (4.54 mg kg ⁻¹)	ED ₃₅ PhAR-DBH-Me (37.13 mg kg ⁻¹)	PhAR-DBH-Me: tramadol (Cis-CI: 18.57:2.27 mg kg ⁻¹)
Albumin/globulin ratio	1.54 ± 0.04	2.17 ± 0.08 ^a	2.12 ± 0.64 ^a	2.09 ± 0.13 ^a
Blood ureic nitrogen/creatinine ratio	36.19 ± 4.44	31.43 ± 1.78	29.63 ± 1.61	29.59 ± 2.38
#C-Ca (mg per 100 mL)	10.10 ± 0.11	9.77 ± 0.16	9.85 ± 0.08	9.91 ± 0.15
#Globulin (g per 100 mL)	2.60 ± 0.03	1.98 ± 0.05 ^a	2.07 ± 0.05 ^a	2.05 ± 0.09 ^a
#Na/K	33.09 ± 0.65	26.57 ± 1.64 ^a	25.70 ± 0.68 ^a	24.13 ± 1.87 ^a
#Urea (mg per 100 mL)	43.22 ± 1.39	44.20 ± 3.15	41.91 ± 1.62	39.16 ± 1.38
#Albumin (g per 100 mL)	4.05 ± 0.08	4.25 ± 0.07	4.31 ± 0.08	4.18 ± 0.11
#Alkaline phosphatase (U per 100 mL)	140.57 ± 12.04	120.85 ± 5.14	119.85 ± 9.45	107.50 ± 6.27
Alanine transaminase (U per 100 mL)	42.28 ± 2.03	39.42 ± 2.56	47.14 ± 6.20	43.18 ± 4.89
Amylase (U per 100 mL)	135.50 ± 4.92	145.00 ± 5.58	146.50 ± 7.81	133.16 ± 6.68
Blood ureic nitrogen (mg per 100 mL)	20.20 ± 0.65	20.65 ± 1.47	19.58 ± 0.76	18.3 ± 0.64
Creatinine (mg per 100 mL)	0.59 ± 0.05	0.66 ± 0.04	0.66 ± 0.01	0.63 ± 0.04
Ca (mg per 100 mL)	10.10 ± 0.14	10.00 ± 0.12	10.15 ± 0.12	10.06 ± 0.21
Glucose (mg per 100 mL)	113.57 ± 6.48	114.57 ± 2.24	114.28 ± 7.05	117.83 ± 5.15
K (mmol per 100 mL)	4.35 ± 0.07	5.23 ± 0.38	5.66 ± 0.16 ^a	6.06 ± 0.48 ^a
Na (mmol per 100 mL)	141.57 ± 0.71	144.00 ± 1.15	142.57 ± 0.84	142.00 ± 1.23
Phosphate (mg per 100 mL)	7.01 ± 0.34	6.75 ± 0.27	6.90 ± 0.13	7.35 ± 0.40
Bilirubin (mg per 100 mL)	0 ± 0	0 ± 0	0 ± 0	0 ± 0
Total protein (g per 100 mL)	6.60 ± 0.08	6.27 ± 0.07	6.45 ± 0.12	6.23 ± 0.11

Mean ± SEM; *n* = 6.

^aStatistically significant difference *vs.* vehicle; *p* < 0.05.

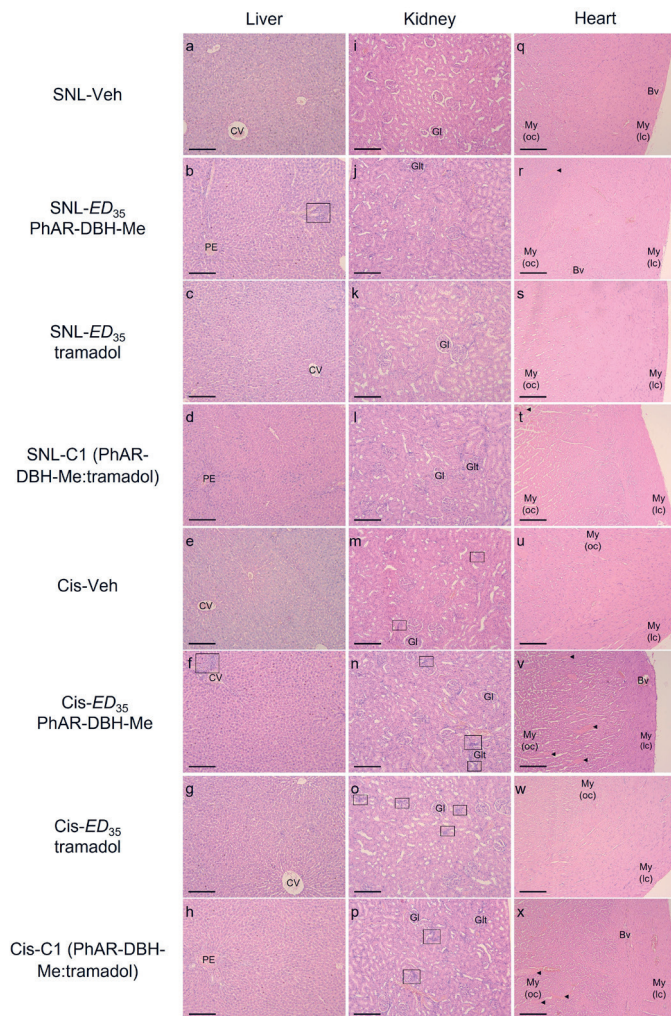


Fig. 3. Representative histological cuts of the liver, kidney, and heart from rats administered with a single effective dose (ED_{35}) of PhAR-DBH-Me ($49.79 \pm 0.05 \text{ mg kg}^{-1}$ and $37.13 \pm 0.06 \text{ mg kg}^{-1}$, for SNL and cisplatin model, resp.) or tramadol ($24.85 \pm 0.05 \text{ mg kg}^{-1}$ and $4.54 \pm 0.6 \text{ mg kg}^{-1}$, for SNL and cisplatin model, resp.) and their combination ($24.88:12.42$, SNL-C1, and $18.57:2.27$, Cis-C1, mg kg^{-1} , PhAR-DBH-Me:tramadol). Illustrative photomicrographs of the liver (a, b, c, d for spinal nerve ligated rats and e, f, g, h for cisplatin-induced rats), kidney (i, j, k, l for spinal nerve ligated rats and m, n, o, p for cisplatin-induced rats) and heart (q, r, s, t for spinal nerve ligated rats and u, v, w, x for cisplatin-induced rats). Tissues stained with hematoxylin and eosin, magnification $10\times$, scale bar = $200 \mu\text{m}$. Images captured by Primo Star Zeiss video camera and analyzed by Zen2 Blue Edition Zeiss program (rectangle – immune cells infiltrate, arrowhead – hemorrhage).

Bv – blood vessel, Cis – cisplatin, CV – central vein, GI – glomeruli, Glt – glomeruli with thickening of Bowman's capsular basement membrane, My (lc) – myocardium (longitudinal cut), My (oc) – myocardium (oblique cut), PE – portal structure

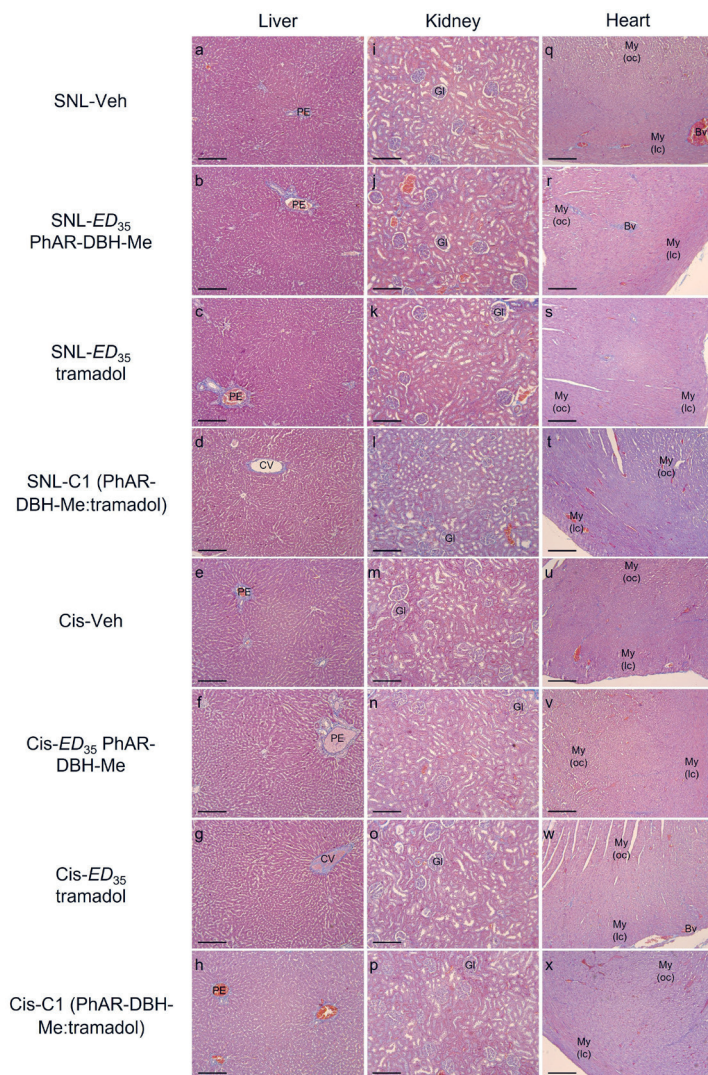


Fig. 4. Collagen structures and their distribution in the liver, kidney and heart from rats administered with a single effective dose (ED_{35}) of PhAR-DBH-Me ($49.79 \pm 0.05 \text{ mg kg}^{-1}$ and $37.13 \pm 0.06 \text{ mg kg}^{-1}$, for SNL and Cis model, resp.) or tramadol ($24.85 \pm 0.05 \text{ mg kg}^{-1}$ and $4.54 \pm 0.6 \text{ mg kg}^{-1}$, for SNL and Cis model, resp.) and their combination ($24.88:12.42$, SNL-C1, and $18.57:2.27$, Cis-C1, mg kg^{-1} , PhAR-DBH-Me:tramadol). Illustrative photomicrographs of the liver (a, b, c, d for spinal nerve ligated rats and e, f, g, h for Cis-induced rats), kidney (i, j, k, l for spinal nerve ligated rats and m, n, o, p for Cis-induced rats) and heart (q, r, s, t for spinal nerve ligated rats and u, v, w, x for Cis-induced rats). Tissues were stained with Masson trichrome, magnification $10\times$, scale bar = $200 \mu\text{m}$; images were taken by Primo Star Zeiss video camera and analyzed by Zen2 Blue Edition Zeiss program.

Cis – cisplatin, CV – central vein, GI – glomeruli, My (lc) – myocardium (longitudinal cut), My (oc) – myocardium (oblique cut), Bv – blood vessel, PE – portal structure

In this regard, it is noteworthy that cisplatin was reported to induce hepatic (42) damage. Nevertheless, those doses were 20 to 50-fold higher than the dose used in cisplatin-induced neuropathy. Notwithstanding, the rats treated with PhAR-DBH-Me displayed a scarce presence of infiltrates of immunological cells around the central vein (Fig. 3f), which did not change the normal structure of the tissue. However, the presence of infiltrates can be related to the metabolism of cannabinoids through CYP450 enzymes (43). PhAR-DBH-Me and Cis-C1 treatments activated CB2 receptors, mainly distributed in immune cells (13, 44). On the contrary, some reports suggest that the pre-treatment with a synthetic agonist of CB2 receptors, in animals with hepatic ischemia, produced a decrease in inflammatory cell infiltration and plasma levels of pro-inflammatory markers (45). On the other hand, the present study showed defined glomeruli with adequate Bowman's space. In addition, kidney samples from SNL (Figs. 3i–l) or cisplatin (Figs. 3m–p) neuropathy rats did not show the presence of hemorrhage, inflammatory infiltrate, and apoptotic or necrotic cells. However, in SNL rats treated with PhAR-DBH-Me (Fig. 3j) or SNL-C1 (Fig. 3l) a decreased Bowman's space in some glomeruli (2–3 per field) was observed, but the normal structure of glomeruli was not affected by this condition. On the other hand, in cisplatin-induced rats, all experimental groups showed the presence of small infiltrates of immunological cells (1–3 per field), without affecting the structure of the renal tissue (Figs. 3n–p).

The toxicological acute assay was extended to the influence on cardiac tissue as well. The absence of lesions (hemorrhage, inflammation, necrosis or apoptotic areas) was observed in the histological analysis of cardiac tissue from tramadol-treated rats, in both SNL (Fig. 3s) and cisplatin (Fig. 3w) groups. However, the rats treated with PhAR-DBH-Me or Cis-C1 presented hemorrhagic areas in the myocardium (oblique cut), which were more widespread and numerous in Cis (Figs. 3v,x) than in PhAR-DBH-Me and SNL-C1 groups (Figs. 3r,t). These findings could be related to vascular damage or vasoconstriction (46), which should be considered in future studies, especially, due to cardiotoxicity reported by some synthetic cannabinoids (47). In this regard, anandamide and synthetic cannabinoids activating CB1 receptors are linked to hemorrhagic shock (47, 48).

Histopathological examination in the liver (Figs. 4a–c in SNL, and Figs. 4e–h in Cis), kidney (Figs. 4i–l in SNL, and Figs. 4m–p in Cis) and heart (Figs 4q–t in SNL, and Figs. 4u–x in Cis) from rats that received the vehicle, tramadol, PhAR-DBH-Me, Cis-C1 or SNL-C1 treatment, did not show alterations for both SNL and Cis animals.

Altogether, biochemical, and histological observations suggested that none of the treatments used in monotherapy or co-administered, in a single dose, produced potential hepatotoxicity, nephrotoxicity or cardiotoxicity. Further, sub- and chronic toxicity assays should be performed to evaluate the effect of PhAR-DBH-Me, tramadol, or their combination on a long-term scale, as well as the pharmacokinetic interaction between both drugs, should be evaluated in a future study.

CONCLUSIONS

PhAR-DBH-Me and tramadol combination has a synergistic antiallodynic effect in spinal nerve ligated rats and an additive antiallodynic effect in Cis-induced neuropathy rats. This synergistic interaction could be due to the activation of CB1, CB2, TRPV1, and opioid receptors, as well as pharmacokinetic interactions. Hence, PhAR-DBH-Me and tramadol combination might be a candidate for a new therapeutic approach in the treatment

of pain. Moreover, acute toxicological assays did not show relevant changes in hepatic, renal or cardiac function. However, the safety profile of this combination on a long-term administration basis needs to be a future scientific task.

Acknowledgments. – We thank Elvis Noguera Corona and Sandra Guadalupe Lugo Apodaca for their technical collaboration in surgery and histology procedures, resp. and Carolina Gabriela Plazas Guerrero for editing English language in the manuscript.

Funding. – This work is part of the postdoctoral appointment of Dra. Geovanna Nallely Quiñonez-Bastidas, partially funded by a fellowship granted by Programa de Becas Postdoctorales from Dirección General de Asuntos del Personal Académico, Universidad Nacional Autónoma de México (DGAPA-UNAM). This work was partially supported by the grants PAIP5000-9143 from Facultad de Química, PAPIIT-IN218320 from Dirección General de Asuntos del Personal Académico, Universidad Nacional Autónoma de México, and Pro-A2-021 from PROFAPI 2022, Universidad Autónoma de Sinaloa.

Conflict of interest. – The authors declare no potential conflict of interest.

Author's contributions. – Quiñonez-Bastidas and Navarrete conceived the idea and participated in design the study. Experiments were conducted by Quiñonez-Bastidas, Osuna-Martínez and Redallicea. Lopez-Ortiz and Regla synthesized PhAR-DBH-Me, whereas that, Quiñonez-Bastidas and Navarrete performed the data analysis. Quiñonez-Bastidas and Osuna-Martínez wrote the manuscript and Navarrete made the pertinent corrections. All authors revised the draft of manuscript.

REFERENCES

1. A. Mohammadkhani and S. L. Borgland, Cellular and behavioral basis of cannabinoid and opioid interactions: Implications for opioid dependence and withdrawal, *J. Neurosci. Res.* **100** (2022) 278–296; <https://doi.org/10.1002/jnr.24770>
2. M. Ghonghadze, K. Pachkoria, M. Okujava, N. Antelava and N. Gongadze, Endocannabinoids receptors mediated central and peripheral effects, *Georgian Med. News* **298** (2020) 137–143.
3. E. E. Bagley and S. L. Ingram, Endogenous opioid peptides in the descending pain modulatory circuit, *Neuropharmacology* **173** (2020) Article ID 108131; <https://doi.org/10.1016/j.neuropharm.2020.108131>
4. G. Corder, D. D. Castro, M. R. Bruchas and G. Scherrer, Endogenous and exogenous opioids in pain, *Annu. Rev. Neurosci.* **41** (2018) 453–473; <https://doi.org/10.1146/annurev-neuro-080317-061522>
5. S. Narouze, Antinociception mechanisms of action of cannabinoid-based medicine: an overview for anesthesiologists and pain physicians, *Reg. Anesth. Pain Med.* **46**(3) (2021) 240–250; <https://doi.org/10.1136/rapm-2020-102114>
6. W. Fujita, I. Gomes and L. A. Devi, Revolution in GPCR signaling: opioid receptor heteromers as novel therapeutic targets: IUPHAR review 10, *Br. J. Pharmacol.* **171**(18) (2014) 4155–4176; <https://doi.org/10.1111/bph.12798>
7. S. Sierra, A. Gupta, I. Gomes, M. Fowkes, A. Ram, E. N. Bobeck, and L. A. Devi, Targeting cannabinoid 1 and delta-opioid receptor heteromers alleviates chemotherapy-induced neuropathic pain, *ACS Pharmacol. Transl. Sci.* **2** (2019) 219–229; <https://doi.org/10.1021/acspsci.9b00008>
8. M. M. Ibrahim, F. Porreca, J. Lai, P. J. Albrecht, F. L. Rice, A. Khodorova, G. Davar, A. Makriyannis, T. W. Vanderah, H. P. Mata and T. P. Malan, CB2 cannabinoid receptor activation produces antinociception by stimulating peripheral release of endogenous opioids, *Proc. Natl. Acad. Sci. USA* **102**(8) (2005) 3093–3098; <https://doi.org/10.1073/pnas.0409888102>
9. S. P. Welch and D. L. Stevens, Antinociceptive activity of intrathecally administered cannabinoids alone, and in combination with morphine, in mice, *J. Pharmacol. Exp. Ther.* **262**(1) (1992) 10–18.

10. F. L. Smith, D. Cichewicz, Z. L. Martin and S. P. Welch, The enhancement of morphine antinociception in mice by delta9-tetrahydrocannabinol, *Pharmacol. Biochem. Behav.* **60**(2) (1998) 559–566; [https://doi.org/10.1016/s0091-3057\(98\)00012-4](https://doi.org/10.1016/s0091-3057(98)00012-4)
11. O. Gunduz, H. C. Karadag and A. Ulugol, Synergistic anti-allodynic effects of nociceptin/orphanin FQ and cannabinoid systems in neuropathic mice, *Pharmacol. Biochem. Behav.* **99**(4) (2011) 540–544; <https://doi.org/10.1016/j.pbb.2011.05.029>
12. J. M. Vigil, S. S. Stith, I. M. Adams and A. P. Reeve, Associations between medical cannabis and prescription opioid use in chronic pain patients: A preliminary cohort study, *PLoS One* **12** (2017) e0187795 (13 pages); <https://doi.org/10.1371/journal.pone.0187795>
13. G. N. Quiñonez-Bastidas, O. Palomino-Hernández, M. López-Ortíz, H. I. Rocha-González, G. M. González-Anduaga, I. Regla and A. Navarrete, Antiallodynic effect of PhAR-DBH-Me involves cannabinoid and TRPV1 receptors, *Pharmacol. Res. Perspect.* **8** (2020) e00663 (12 pages); <https://doi.org/10.1002/prp2.663>
14. M. Lopez-Ortiz, A. Herrera-Solis, A. Luviano-Jardon, N. Reyes-Prieto, I. Castillo, I. Monsalvo, P. Demare, M. Méndez-Díaz, I. Regla and O. Prospero-García, Chemoenzymatic synthesis and cannabinoid activity of a new diazabicyclic amide of phenylacetylricinic acid, *Bioorg. Med. Chem. Lett.* **20**(11) (2010) 3231–3234; <https://doi.org/10.1016/j.bmcl.2010.04.074>
15. S. H. Kim and J. M. Chung, An experimental model for peripheral neuropathy produced by segmental spinal nerve ligation in the rat, *Pain* **50** (1992) 355–363; [https://doi.org/10.1016/0304-3959\(92\)90041-9](https://doi.org/10.1016/0304-3959(92)90041-9)
16. N. Authier, J. P. Gillet, J. Fialip, A. Eschaliere and F. Coudore, An animal model of nociceptive peripheral neuropathy following repeated cisplatin injections, *Exp. Neurol.* **182**(1) (2003) 12–20; [https://doi.org/10.1016/s0014-4886\(03\)00003-7](https://doi.org/10.1016/s0014-4886(03)00003-7)
17. S. R. Chaplan, F. W. Bach, J. W. Pogrel, J. M. Chung and T. L. Yaksh, Quantitative assessment of tactile allodynia in the rat paw, *J. Neurosci. Meth.* **53**(1) (1994) 55–63; [https://doi.org/10.1016/0165-0270\(94\)90144-9](https://doi.org/10.1016/0165-0270(94)90144-9)
18. R. J. Tallarida, *Drug Synergism and Dose-Effect Data Analysis*, in *Drug Synergism and Dose-Effect Data Analysis*, 1st ed., Chapman and Hall/CRC, New York 2000.
19. J. Balderas-López, A. Navarrete and A. Alfaro, *Graded Dose-Response Curves*, in *Pharmacometrics*, 1st ed., Universidad Nacional Autónoma de México, Mexico City 2017.
20. S. Goutelle, M. Maurin, F. Rougier, X. Barbaut, L. Bourguignon, M. Ducher and P. Maire, The Hill equation: a review of its capabilities in pharmacological modelling, *Fundam. Clin. Pharmacol.* **22**(6) (2008) 633–648; <https://doi.org/10.1111/j.1472-8206.2008.00633.x>
21. S. de J. Acosta-Cota, E. M. Aguilar-Medina, R. Ramos-Payána, J. G. Rendón Maldonado, J. G. Romero-Quintana, J. Montes-Avila, J. I. Sarmiento-Sánchez, C. G. Plazas-Guerrero, M. J. Vergara-Jiménez, A. Sánchez-López, D. Centurión and U. Osuna-Martínez, Therapeutic effect of treatment with metformin and/or 4-hydroxychalcone in male Wistar rats with nonalcoholic fatty liver disease, *Eur. J. Pharmacol.* **863** (2019) Article ID 172699 (14 pages); <https://doi.org/10.1016/j.ejphar.2019.172699>
22. R. A. Gibson, J.-A. Lim, S. J. Choi, L. Flores, L. Clinton, D. Bali, S. Young, A. Asokan, B. Sun and P. S. Kishnani, Characterization of liver GSD IX γ 2 pathophysiology in a novel *Phkg2^{-/-}* mouse model, *Mol. Genet. Metab.* **133**(3) (2021) 269–276; <https://doi.org/10.1016/j.ymgme.2021.05.008>
23. N. P. Kazantzis, S. L. Casey, P. W. Seow, V. A. Mitchell and C. W. Vaughan, Opioid and cannabinoid synergy in a mouse neuropathic pain model, *Br. J. Pharmacol.* **173**(16) (2016) 2521–2531; <https://doi.org/10.1111/bph.13534>
24. M. Déciga-Campos, P. M. Ramírez-Marín and F. J. López-Muñoz, Synergistic antinociceptive interaction between palmitoylethanolamide and tramadol in the mouse formalin test, *Eur. J. Pharmacol.* **765** (2015) 68–74; <https://doi.org/10.1016/j.ejphar.2015.08.025>

25. L. Roulet, V. Rollason, J. Desmeules and V. Piguet, Tapentadol versus tramadol: A narrative and comparative review of their pharmacological, efficacy and safety profiles in adult patients, *Drugs* **81** (2021) 1257–1272; <https://doi.org/10.1007/s40265-021-01515-z>
26. N. T. Snider, M. J. Sikora, C. Sridar, T. J. Feuerstein, J. M. Rae and P. F. Hollenberg, The endocannabinoid anandamide is a substrate for the human polymorphic cytochrome P450 2D6, *J. Pharmacol. Exp. Ther.* **327**(2) (2008) 538–545; <https://doi.org/10.1124/jpet.108.141796>
27. N. T. Snider, J. A. Nast, L. A. Tesmer and P. F. Hollenberg, A cytochrome P450-derived epoxy-generated metabolite of anandamide is a potent cannabinoid receptor 2-selective agonist, *Mol. Pharmacol.* **75**(4) (2009) 965–972; <https://doi.org/10.1124/mol.108.053439>
28. M. Pratt-Hyatt, H. Zhang, N. T. Snider and P. F. Hollenberg, Effects of a commonly occurring genetic polymorphism of human CYP3A4 (I118V) on the metabolism of anandamide, *Drug Metab. Dispos.* **38**(11) (2010) 2075–2082; <https://doi.org/10.1124/dmd.110.033712>
29. M. Vázquez, N. Guevara, C. Maldonado, P. C. Guido and P. Schaiquevich, Potential pharmacokinetic drug-drug interactions between cannabinoids and drugs used for chronic pain, *Biomed. Res. Int.* **2020** (2020) Article ID 3902740 (9 pages); <https://doi.org/10.1155/2020/3902740>
30. J. Guindon, Y. Lai, S. M. Takacs, H. B. Bradshaw and A. G. Hohmann, Alterations in endocannabinoid tone following chemotherapy-induced peripheral neuropathy: effects of endocannabinoid deactivation inhibitors targeting fatty-acid amide hydrolase and monoacylglycerol lipase in comparison to reference analgesics following cisplatin treatment, *Pharmacol. Res.* **67**(1) (2013) 94–109; <https://doi.org/10.1016/j.phrs.2012.10.013>
31. H. L. Blanton, J. Brelsfoard, N. DeTurk, K. Pruitt, M. Narasimhan, D. J. Morgan and J. Guindon, Cannabinoids: Current and future options to treat chronic and chemotherapy-induced neuropathic pain, *Drugs* **79** (2019) 969–995; <https://doi.org/10.1007/s40265-019-01132-x>
32. D. da Fonseca Pacheco, A. Klein, A. P. de Castro, C. M. da Fonseca Pacheco, J. N. de Francischi and I. D. G. Duarte, The mu-opioid receptor agonist morphine, but not agonists at delta- or kappa-opioid receptors, induces peripheral antinociception mediated by cannabinoid receptors, *Br. J. Pharmacol.* **154**(5) (2008) 1143–1149; <https://doi.org/10.1038/bjp.2008.175>
33. B. Wiese and A. R. Wilson-Poe, Emerging evidence for cannabis' role in opioid use disorder, *Cannabis Cannabinoid Res.* **3**(1) (2018) 179–189; <https://doi.org/10.1089/can.2018.0022>
34. N. Petejova and A. Martinek, Acute kidney injury following acute pancreatitis: A review, *Biomed. Pap. Med. Fac. Univ. Palacky Olomouc Czech Repub.* **157**(2) (2013) 105–113; <https://doi.org/10.5507/bp.2013.048>
35. J. Zaias, M. Mineau, C. Cray, D. Yoon and N. H. Altman, Reference values for serum proteins of common laboratory rodent strains, *J. Am. Assoc. Lab. Anim. Sci.* **48**(4) (2009) 387–390.
36. J. S. Hochman and N. Q. Brill, Chronic marijuana usage and liver function, *Lancet* **298**(7728) (1971) 818–819; [https://doi.org/10.1016/s0140-6736\(71\)92771-1](https://doi.org/10.1016/s0140-6736(71)92771-1)
37. L. E. Ewing, C. M. Skinner, C. M. Quick, S. Kennon-McGill, M. R. McGill, L. A. Walker, M. A. ElSohly, B. J. Gurley and I. Koturbash, Hepatotoxicity of a cannabidiol-rich cannabis extract in the mouse model, *Molecules* **24**(9) (2019) Article ID 1694 (17 pages); <https://doi.org/10.3390/molecules24091694>
38. Y.-C. Hsu, C.-C. Lei, Y.-H. Shih, C. Ho and C.-L. Lin, Induction of proteinuria by cannabinoid receptors 1 signaling activation in CB1 transgenic mice, *Am. J. Med. Sci.* **349**(2) (2015) 162–168; <https://doi.org/10.1097/MAJ.0000000000000352>
39. E. C. Morais Rateke, C. Matiollo, E. Q. de Andrade Moura, M. Andrigueti, C. Maccali, J. S. Fonseca, S. M. F. Canova, J. L. Narciso-Schiavon and L. L. Schiavon, Low sodium to potassium ratio in spot urine sample is associated with progression to acute kidney injury and mortality in hospitalized patients with cirrhosis, *Dig. Liver Dis.* **53**(9) (2021) 1159–1166; <https://doi.org/10.1016/j.dld.2020.12.117>

40. M. Boada, A. Pippo, M. Rodriguez-Milhomens, V. González, R. Higgie, V. Mérola, J. M. Carissi and R. Silviriño, Hiperpotasemia severa en emergencia: Manifestaciones clínicas y manejo terapéutico a propósito de tres casos [Severe hyperkalemia in emergency: Clinical manifestations and therapeutic management of three cases], *Arch. Med. Int.* **34** (2012) 91–94.
41. Y. Koura, A. Ichihara, Y. Tada, Y. Kaneshiro, H. Okada, C. J. Temm, M. Hayashi and T. Saruta, Anandamide decreases glomerular filtration rate through predominant vasodilation of efferent arterioles in rat kidneys, *J. Am. Soc. Nephrol.* **15**(6) (2004) 1488–1494; <https://doi.org/10.1097/01.asn.0000130561.82631.bc>
42. J. S. Kim, J. Y. Son, K. S. Kim, H. J. Lim, M.-Y. Ahn, S. J. Kwack, Y.-M. Kim, K. Y. Lee, J. Lee, B. M. Lee and H. S. Kim, Hepatic damage exacerbates cisplatin-induced acute kidney injury in Sprague-Dawley rats, *J. Toxicol. Environ. Health A* **81**(11) (2018) 397–407; <https://doi.org/10.1080/15287394.2018.1451179>
43. C. J. Lucas, P. Galettis and J. Schneider, The pharmacokinetics and the pharmacodynamics of cannabinoids, *Br. J. Clin. Pharmacol.* **84**(11) (2018) 2477–2482; <https://doi.org/10.1111/bcp.13710>
44. P. Pacher and R. Mechoulam, Is lipid signaling through cannabinoid 2 receptors part of a protective system?, *Prog. Lipid. Res.* **50** (2011) 193–211; <https://doi.org/10.1016/j.plipres.2011.01.001>
45. M. Rajesh, H. Pan, P. Mukhopadhyay, S. Bátkai, D. Osei-Hyiaman, G. Haskó, L. Liaudet, B. Gao and P. Pacher, Cannabinoid-2 receptor agonist HU-308 protects against hepatic ischemia/reperfusion injury by attenuating oxidative stress, inflammatory response, and apoptosis, *J. Leukoc. Biol.* **82**(6) (2007) 1382–1389; <https://doi.org/10.1189/jlb.0307180>
46. J. S. Richter, V. Quenardelle, O. Rouyer, J. S. Raul, R. Beaujeux, B. Gény and V. Wolff, A systematic review of the complex effects of cannabinoids on cerebral and peripheral circulation in animal models, *Front. Physiol.* **9** (2018) Article ID 622 (13 pages); <https://doi.org/10.3389/fphys.2018.00622>
47. P. Pacher, S. Steffens, G. Haskó, T. H. Schindler and G. Kunos, Cardiovascular effects of marijuana and synthetic cannabinoids: the good, the bad, and the ugly, *Nat. Rev. Cardiol.* **15** (2018) 151–166; <https://doi.org/10.1038/nrcardio.2017.130>
48. J. A. Wagner, K. Varga, E. F. Ellis, B. A. Rzigalinski, B. R. Martin and G. Kunos, Activation of peripheral CB1 cannabinoid receptors in haemorrhagic shock, *Nature* **390**(6659) (1997) 518–521; <https://doi.org/10.1038/37371>